Cache-Aided Millimeter Wave Ad-Hoc Networks with Contention-Based Content Delivery

Satyanarayana Vuppala, *Member, IEEE*, Thang X. Vu, *Member, IEEE*, Sumit Gautam, *Student Member, IEEE* and Symeon Chatzinotas, *Senior Member, IEEE* and Björn Ottersten, *Fellow, IEEE*

***Abstract*—The narrow-beam operation in millimeter wave (mmWave) networks minimizes the network interference leading to a noise-limited networks in contrast with interference-limited ones. The medium access control (MAC) layer throughput, and interference management strategies heavily depend on the noise-limited or interference-limited regime. Yet, these regimes are not considered in recent mmWave MAC layer designs, which can potentially have disastrous consequences on the communication performance. In this paper, we investigate the performance of cache-enabled MAC based mmWave ad-hoc networks, where randomly distributed nodes are supported by a cache. The ad-hoc nodes are modeled as homogenous Poisson Point Processes (PPP). Specifically, we study the optimal content placement (or caching placement) at desirable mmWave nodes using a network model that accounts for uncertainties both in node locations and blockages. We propose a contention-based multimedia delivery protocol to avoid collisions among the concurrent transmissions. Subsequently, only the node with smallest back-off timer amongst its contenders is allowed to transmit. We then characterize the average success probability of content delivery. We also characterize the cache hit ratio probability, and transmission probability of this system under essential factors, such as blockages, node density, path loss and caching parameters.**

***Index Terms*—Blockages, caching, interference, medium access control, millimeter-wave networks, Poison point processes**

I. Introduction

THE key objectives of future generation wireless communication systems include billions of connected devices, data rates in the range of Gbps, lower latencies, improved coverage and environment-friendly, low-cost, and energy efficient operations. High user mobility is one of the expectations of such future communication networks where the increase in the demand of content is primarily due to data applications like high quality video streaming and social networks. Mobile video traffic accounted for 55% of total mobile traffic in 2016 because video content on smart mobile devices requires higher data rates compared to any other mobile data services. According to Cisco's annual report, mobile video traffic is expected to generate 74% of the global mobile data traffic by 2020 [1]. On the other hand, the existing cellular spectrum is approaching its performance limits thus giving birth to the growing interest in and exploration of supplementary resources to meet these demands [2]. As a result, millimeter wave (mmWave) frequencies are being investigated to serve as an alternative or provide assistance to the existing technologies.

To meet the goals of the vision of future wireless systems, cache-enabled network architectures have been investigated and projected as the possible solution to the inevitable data tsunami in coming years. The key idea in these systems is to avail the assistance from helper nodes instead of cellular infrastructures to successfully deliver the desired content to the end-user devices. Helper nodes are generally categorised as small base stations (SBSs) [3] and user mobile devices that are used for ad-hoc communications. In such networks, a user's mobile device caches a number of popular video files based on the available storage and a particular caching policy that is utilised and controlled by a central entity. Then, it can serve other users who request the cached files via device-to-device (D2D) communications [4].

On the other hand, in recent past, mmWave use was limited to radar communication [5]. Due to higher frequencies, the path losses are higher and blockage is more severe due to their smaller wavelengths. This was the reason why mmWave technology was discarded concerning its application in mobile communication. Nonetheless, high gain antenna arrays have been designed which can potentially overcome the losses. In fact, wireless systems with high data rates measured in gigabits-per-second have been implemented for indoor applications [6]. The work in [7] explores the sparsity that characterises mmWave to develop the precoding or combining solution that achieves near optimal spectral efficiency. Tractable models for backhauled links and per user rates have been studied in [8] and [9], using stochastic geometry for their analysis.

The deployment of small cells is a key method by which wireless communication is expected to evolve as the next generation of networks [10]. MmWave transmission by nature can be deployed into ad-hoc mode due to its limited range of propagation. The work in [11] provides the coverage analysis of such mmWave ad-hoc networks whereas [12] provides coverage analysis in densification of mmWave cells. In addition, researchers are looking into how to maximize content delivery in networks to increase the users' quality of experience (QoE) [13]. Moreover, *mmWave communication in ad-hoc networks can exploit the directionality* to minimize the network interference. In addition, it provides high spectral efficiency for content delivery. To this end, *from the perspective of such mmWave networks, we demonstrate the effectiveness of off-line caching with respect to blockages*.

The idea of caching in mobile networks is triggering research interest as a promising approach to increase user

The authors are with Interdisciplinary Centre for Security, Reliability and Trust, University of Luxembourgh, 29, Avenue J.F Kennedy, L-1855 Luxembourg. E-mails: {satyanarayana.vuppala; thang.vu; sumit.gautam; symeon.chatzinotas; bjorn.ottersten}@uni.lu. Corresponding author: S. Vuppala.

This work has received funding from the European Research Council (ERC) under the European Union's Horizon H2020 research and innovation programme (grant agreement No 742648).

satisfaction as well as reducing the cost of backhaul load. Caching has been used to maintain internet traffic over the last two decades and has been largely computer based [14], [15]. A spontaneous reload cache system was introduced in [16] to show that it is possible to have systems with active caches without increasing the hardware overload. This has triggered interest in the formulation of active caches for cellular networks. To this point, authors in [17] applied the content caching approaches to content delivery networks (CDN). Following this direction, [18] showed the role of proactive caching on the network edge to help reducing traffic congestion in the backhaul links. In particular, authors show the effectiveness of proactive caching reducing congestion in the backhaul links wherein both spatial and social structures of networks has been considered to show that proactive caching aids users satisfaction. Subsequently, caching strategies were investigated with various network objectives, including coded caching in wireless networks [19], [20], content caching in heterogeneous networks [21], [22] and D2D caching in [4].

Furthermore, video streaming based cellular caching architectures in cooperation with D2D communications have been investigated in a variety of scenarios over the recent years. Information theoretic bounds for single-hop D2D caching networks are obtained in [4] under arbitrary demand for certain deterministic and random caching policies. In such systems, content can be placed on collaborative nodes formerly, either according to a predefined policy [23], or more intelligently, according to statistics of the user devices' interests [24]. Stochastic geometric based analysis is presented in [25] for the scenario of BSs located in the Euclidian plane. The work in [26] shows that popularity based caching gives better results in terms of outage probability than uniform caching where the BSs cache content randomly irrespective of the popularity. The authors in [27] have investigated the influence of mobility from the perspective of cached enabled D2D networks.

Content placement is a key factor that determines the success of a caching system, and researchers are looking into the optimal way of cache placement for various networks. In this direction, the work in [28] proposes that maximizing the number of active links (the link between two devices is active if one requests a file already cached by the other device) is the optimal transmitting method. Recently in [29], a content placement that balances the reduction of network interference with channel selection diversity is proposed. Following this trend, the authors in [30], [31] studied the optimal geographic content placement problem for D2D networks in which the content popularity follows the Zipf law. In this direction, [32] studied probabilistic caching placement in stochastic wireless D2D caching networks with two objectives: maximizing the cache hit probability and maximizing the cache-aided throughput that is defined by the density of successfully served user requests. All these previous works on caching have focused on transmission at sub 6 GHz frequencies. More recently, the throughput-outage tradeoff of the mmWave link underlying D2D networks under a simplified grid topology is derived in [33] for various caching policies. To this end, in [34], authors proposed a novel policy for device caching that facilitates popular content exchange through high-rate D2D mmWave communication. We would like to state that, though there has been extensive ongoing research on wireless caching, to the best of our knowledge cache aided mmWave systems has not been characterized well enough in recent literature. Thus, in this work, *we study the content placement in mmWave networks where randomly located mmWave nodes store contents probabilistically and independently*.

However, we cannot get away from the fact that these PPP based content caching approaches [25], [26], [29], [32] may not be suitable for real world deployments. Consider a Wireless Fidelity (WiFi) network where all the nodes follow a terrain according to its coverage. Hence, the distribution of nodes is far from being spatially uniform. Such a distribution is clearly distinct from the PPP based network assumptions which leads to a non-Poisson number of nodes per unit area. To model such kind of dependencies between the BSs in cellular networks, recent works [35]–[38] extend the PPP framework to non-Poisson point processes. The recent work in [35] introduced a Ginibre point process (GPP) framework for the analysis of wireless cellular networks where the nodes exhibit repulsion. Following this direction, the authors in [36] analyze the sampling and reconstruction of finite-energy signals in $\mathbb{R}^d$ when the samples are gathered in space according to a determinantal point process whose second order product density function generalizes to $\mathbb{R}^d$ in contrast to a modified GPP in $\mathbb{R}^2$. In [37], the authors propose an approach to using the Gauss-Poisson processes (GuPP) to model spatial distribution of wireless networks, and investigate the benefits of cooperative communications in such GuPP based network. Following these footprints [37], the authors in [38] consider the GuPP for analyzing the effects of nodes' attraction (i.e., opposite of repulsion) on random sampling and signal reconstruction. To this end, the distribution of nodes in the ad-hoc network are completely random, the replusion or attraction may have less impact on the distribution of nodes. In this paper, we consider such an ad-hoc network to facilitate tractability in the analysis.

In addition, interference management is another important aspect that needs special consideration while modeling the mmWave networks. Elaborate interference management schemes enable effective spatial reuse, thereby improving the overall performance of cache-enabled mmWave networks significantly. It is noteworthy that the issue of interference management has not been investigated widely in [8], [9], [11]. Recently, the authors in [39] and [40] have addressed and characterized the interference management issue from the perspective of medium access control (MAC). Distinctly from [8], [9], [11], and leveraging the results from [40], a contention based multimedia delivery protocol is proposed herein to tackle the problem of interference management.

The main contributions of this paper are fivefold, listed as follows

- In order to study the performance of mmWave ad-hoc cache enabled networks, we develop an analytical framework for contention based multimedia delivery assuming a homogeneous Poisson Point Process (PPP) model of ad-hoc nodes with caching ability. Besides, a Zipf distribution is considered to categorize the popularity of the multimedia files.

- Next, we maximize the cache hit probability, the probability that the typical user's request can be served by its neighbor nodes, by *investigating the optimal content placement in this mmWave ad-hoc network*. Consequently, we characterize the average success probability of content delivery.
- We propose a contention based multimedia delivery protocol to avoid collisions among the concurrent transmissions during the delivery phase. We measure *the transmission probability of the transmitter under the proposed contention based multimedia protocol* by applying mathematical tools from stochastic geometry. Therein we characterize the spatial distribution of the active ad-hoc transmitters based on this result.
- Then, we derive the conditional distribution of the point process formed by the active ad-hoc transmitters for a given typical receiver at the origin. Noticiably, the point process formed by the active ad-hoc nodes do not follow a homogeneous PPP due to the contentions among the concurrent transmissions and an infeasibility is introduced for a complete characterization of its spatial distribution. The determination of a Laplace transform of the corresponding aggregate interference from the active ad-hoc nodes becomes challenging. To tackle this difficulty, *we make an approximation to characterize the average success probability of content delivery.*
- Finally, we provide useful guidelines for proper modeling of the resource allocation and interference management protocols for future mmWave networks with a detailed analysis of contention delivery protocol which clarifies the collision level and the throughput performance of mmWave networks.

Note that the work presented without MAC contention in this paper gives the required initial analyses, while reiterating some very important results, that can be considered as a cornerstone for future works in this field. In this paper, contrast to the conventional cache hit optimization in cache-enabled mmWave based wireless networks, we consider an alternative optimization approach for the probabilistic caching placement in mmWave aided caching networks taking into account the blockages.

The rest of the paper is organized as follows. Section II describes the system model. The cache hit ratio and the average successful content delivery probabilities are presented in Section III. In Section IV, we analyze the system with respect to the proposed contention based MAC protocol. Section V gives the numerical results followed by the conclusion in Section VI.

II. System Model

A. Network model

Consider a cache enabled wireless network where mmWave based transmitter nodes are modelled as a two dimensional homogeneous PPP Φ with intensity λ, each associated to a receiver as shown in Fig. 1. For simplicity, we refer the receiver and the transmitter of the typical link as the typical receiver and the tagged transmitter respectively. Each node contains storage units that are used to cache popular files. We refer to these units as the local caches. In addition, a central source containing a global cache consisting of all the files a user would require, is accessible to all the nodes in this network via wired backhaul links. This is to cater for the scenarios when the local caches do not contain the requested files.

Assumption 1: We assume that the typical receiver is associated to a transmitter which does not store the requested content. Therefore, the receiver seeks the desired content from its nearest available transmitter. It is important to note that when a receiver requests for a file, it is served either by the nearest line-of-sight (LOS) node or the best LOS node that has the best average received power.

Using Slivnyaks Theorem [41], it is found that for a given typical transmitter-receiver at the origin, the conditional distribution of the potential interferers (all transmitters excluding the tagged transmitter) is another homogeneous PPP with the same density λ. We assume that a receiver can decode at least one of the multiple transmissions from various neighbours that intend to communicate with it. This reasonable assumption has been considered for the performance evaluation in [8], [9], [11], [12] and is propelled by the shortage of multiuser detection in many devices including the ones with mmWave technology. Considering the receiver of the typical link, all other transmitters in the network acts as potential interferers to the typical receiver. This interference level depends on the density and location of the interferers relative to the typical receiver, transmission powers, channel model, antenna radiation pattern, blockage model, and transmission and reception beamwidths.

Collision model:

In this paper, we consider a slotted ALOHA protocol[1] [39], [40] without power control to obtain a lower bound on its performance, which leads to the the transmission power of P_m available to all the links. Assuming an active probability of every transmitter (interferer) as ρ, we define the probability of active transmission in each time interval as ρ_a. We exploit the property of the slotted ALOHA that the outset of the transmissions are regulated at the beginning of a time slot. In addition, considering the worst case analysis of an ad-hoc network with a cellular system, the slotted ALOHA is found to be a good choice of protocol models. This is due to the fact that the devices are synchronous by utilizing the synchronization signals from the BS.

In the content delivery phase, we assume that each request by an ad-hoc node starts with a random back-off timer following a uniform distribution in the limits [0 1]. This assumption facilitates collision avoidance among the concurrent transmissions. Prior to the expiration of its back-off timer, the transmitter monitors the medium and then decides to commence its transmissions in case there is no contender detection

[1]The current analysis of this paper can be extended to the pure ALOHA and Carrier-sense multiple access (CSMA) cases. However, we restrict our analysis to slotted ALOHA case for analytical tractability.

TABLE I
NOTATIONS

Notation	Description
Φ	Poisson Point Process (PPP)
λ	Density of the PPP
$\mho$	Contention threshold
ρ_a	Probability of active transmission
β	Density of blockages
R_d	Nearest node distance
$d_{\max}$	Maximum communication range
G^M	Main lobe (M) antenna gain
G^m	Side lobe (m) antenna gain
ς_{lk} $l,k \in \{\mathrm{M},\mathrm{m}\}$	Antenna gain probability
Θ_j	SINR threshold for a given file j
α	Path loss exponent
H_m	Fading power random variable
ν	Nakagami fading parameter
P	Node transmit power
$\mathcal{L}$	Library of contents
$\mathcal{M}$	Cache size
Υ	Zipf exponent
f_j	Content request probability of j-th file
q_j	Content placement probability of j-th file

with contention threshold $\mho$; while this defers otherwise. In other words, considering the content delivery phase under the suggested contention based multimedia protocol, we propose that a transmitter under the request is allowed to transmit only if it has the minimal back-off timer among its contenders with contention threshold $\mho$.

Assumption 2: For any two available transmitters x_i and x_j, we say that the latter is a contender of the former with a contention threshold $\mho$, only if $P_m G_l H_m |x_j - x_i|^{-\alpha_m} \geq \mho$; where G_l is the mmWave directivity gain, H_m is the fading power between the two corresponding transmitters and α_m is the path loss exponent.

We additionally incorporate the interference protocol model [42], as it is commonly used in the context of MAC layer analysis [42], [43]. According to this model, a collision occurs between a reference receiver and its intended transmitter for a given distance if there is another interfering transmitter placed no further than a certain distance from the reference receiver. In this context, we hereafter refer to this interference range as $d_{\max}$[2], which is defined as the maximum distance between an interferer and the receiver causing a probable collision or an outage.

In particular, we propose a contention based multimedia delivery protocol with contention threshold $\mho$ in order to avoid collisions among the concurrent transmissions. Under this design, a content request from the typical receiver can be served iff:

(a) the tagged transmitter is operational and active;

[2]Besides its simplicity, the recent investigation in [40] reveals that the special characteristics of mmWave networks makes such interference model quite accurate.

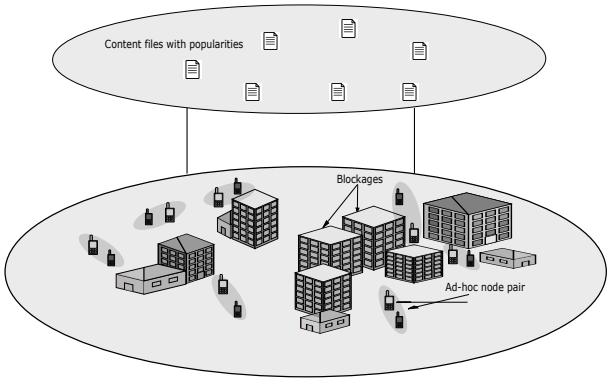

Fig. 1. An illustration of a network modeled by an overlay of ad-hoc nodes and blockages.

(b) the typical receiver falls within the LOS of the tagged transmitter;
(c) the desired file is present in the cache of the tagged transmitter within a radius of R_d;
(d) the tagged transmitter is aligned with receiver[3];
(e) the tagged transmitter is within the maximum range[4] of communication $d_{\max}$;
(f) at least one of the accessible transmitters has the minimal back-off timer among its contenders with contention threshold $\mho$;

Blockage model: MmWaves are susceptible to blockages making it imperative to model blockages for true representation of practical mmWave systems. Blockages in the network are usually concrete buildings. We consider the blockages to be stationary blocks which are invariant with respect to direction. We leverage the concept of the blockage model from [44], and accordingly, consider a two state statistical model for each link. The link can be either LOS or non-line-of-sight (NLOS); LOS link occurs when there is a direct propagation path between the transmitter and the receiver, while NLOS occurs when the link is blocked and the receiver receives the signal through reflection from a blockage. Let the LOS link be of length r, then the probabilities of occurrence $p_{\mathrm{L}}(.)$ and $p_{\mathrm{N}}(.)$ of LOS and NLOS states respectively can be given as a function of r as

$$p_{\mathrm{L}}(r) = e^{-\beta r}, \quad p_{\mathrm{N}}(r) = 1 - e^{-\beta r}, \tag{1}$$

where β is the blockage density.

Beamforming model: Directional beamforming is implemented at both transmitters and receivers for cross communication in this system. The beam patterns are approximated to the sectorized gain patterns as in [11]. Let θ be the beamwidth of the main lobe. Then the antenna gain pattern for a transmit or receive node about an angle ϕ is given as

$$G_q(\theta) = \left\{ \begin{array}{ll} G_q^{\mathrm{M}} & \text{if} |\phi| \leq \theta \\ G_q^{\mathrm{m}} & \text{if} |\phi| \geq \theta \end{array} \right\}, \tag{2}$$

[3]Due to high delivery requirements, we assume that the intended transmitter is aligned with the receiver. Then, the transmitter and its associated receiver have a perfect channel knowledge, and then adjust their steering orientation so as to achieve the maximum directionality gain. Therefore, on such occasions, we only consider the main lobe - main lobe effect in the subsequent analysis.

[4]It is noteworthy that $R_d < d_{\max}$.

where $q \in \mathrm{T}, \mathrm{R}$ (T denotes the transmitter, and R the receiver), $\phi \in [0, 2\pi)$ is the angle of boresight direction, G_q^{M} and G_q^{m} are the array gains of main and side lobes respectively.

The effective antenna gain for an interferer as seen by the typical receiver will depend on the directivity gains of the main (i.e., G^{M}) and side (i.e., G^{m}) lobes of the antenna beam pattern and is expressed as

$$G_i = \left\{ \begin{array}{ll} G^{\mathrm{M}}G^{\mathrm{M}}, & \varsigma_{\mathrm{MM}} = (\frac{\theta}{2\pi})^2 \\ G^{\mathrm{M}}G^{\mathrm{m}}, & \varsigma_{\mathrm{Mm}} = \frac{\theta(2\pi-\theta)}{(2\pi)^2} \\ G^{\mathrm{m}}G^{\mathrm{M}}, & \varsigma_{\mathrm{mM}} = \frac{\theta(2\pi-\theta)}{(2\pi)^2} \\ G^{\mathrm{m}}G^{\mathrm{m}}, & \varsigma_{\mathrm{mm}} = (\frac{2\pi-\theta}{2\pi})^2 \end{array} \right\}, \tag{3}$$

where ς_{lk}, with $l, k \in \{\mathrm{M}, \mathrm{m}\}$, denotes the probability that the antenna gain $G^l G^k$ is observed at the receiver. Thus, the effective gain can be considered as a random variable, which can take any of the above mentioned values. Further, we assume that the transmitter of every link is spatially aligned[5] with its intended receiver as considered in [44].

Channel model: For analytical tractability, we consider Nakagami fading model as it is commonly used in the literature [11], [44]. Hence, the channel power is distributed according to

$$H_m \sim f_{H_m}(x;\nu) \triangleq \frac{\nu^\nu x^{\nu-1} e^{-\nu x}}{\Gamma(\nu)}, \tag{4}$$

where ν is the Nakagami fading parameter and $\Gamma(\nu)$ is the gamma function.

For simplicity, we represent the size of a cache by the size of its library, that is the total number of contents in the library is L and bit rate of Θ bits/s/Hz. Thus, the set of contents is denoted as $\mathcal{L} = \{1, 2, 3, \ldots, L\}$. The more popular contents in the library with L contents are requested with a higher likelihood.

Caching model: The requests from nodes to the tagged transmitters are assumed to be independent of each other. Let f_j be the probability that a user requests the j-th file in the library. This probability is defined according to Zipf distribution [45] as

$$f_j = \frac{\frac{1}{j^\Upsilon}}{\sum_{i=1}^{L} \frac{1}{i^\Upsilon}}, \quad 1 \le j \le L, \tag{5}$$

where Υ is the Zipf exponent which controls the popularity of files with large values of Υ indicating a higher content reuse.

We assume random content placement where the node stores or caches the content j with probability q_j for all requested files, i.e., $\forall j \in \mathcal{L}$. Consider $\mathbf{q} = [q_1, \cdots, q_L]$ as the caching probabilities of the file $i \in [1, L]$, and constraint is $\sum_{j=1}^{L} q_j \le \mathcal{M}$. Readers are encouraged to refer [46] for more details on random content placement. Under the assumption of content request or overhearing, each content is cached at transmitter node in probabilistic way. The transmitter nodes storing the content j can be modeled as an independent PPP with intensity $q_j\lambda$, where the locations of all transmitter nodes storing the content j are denoted by Φ_j.

Consider an event when the file requested by the receiver is not cached in the given tagged transmitter. With such an assumption, we now define two types of cache hit events as follows

- *Case 1: nearest node*, when the requested file is cached at the nearest LOS mmWave transmitter node.
- *Case 2: best node*, when the requested file is not found in any of the nearby mmWave LOS transmitter nodes (i.e., based on distance) but in one of its best LOS transmitter nodes with the least average received path loss. This is solely based on the transmitter node with the largest path gain of the received signal.

The proposed cache hit events are distinct from each other since the best node scenario depends on the channel conditions while the nearest node scenario relies only on the distance between the concerned nodes.

B. Performance metrics

The metric that we consider in this paper, is the average success probability which is defined forthwith.

Let $\Phi_j^c (\triangleq \Phi \backslash \Phi_j)$ be another set of interfering locations with density $(1-q_j)\lambda$, i.e., interference from all other ad-hoc nodes which do not cache content j in their cache. Therefore, the received SINR for the typical receiver can now be defined as

$$\bar{\zeta_j} \triangleq \frac{P_m G_l |h_l|^2 {r_l}^{-\alpha_m}}{\sigma^2 + \sum\limits_{i \in \Phi_j} P_m G_i |h_i|^2 r_i^{-\alpha_m} + \sum\limits_{i \in \Phi_j^c} P_m G_i |h_i|^2 r_i^{-\alpha_m}}, \tag{6}$$

where G_l is the antenna array gain function, h_l is the fading gain at the receiver of interest, r_l is the link length, σ^2 is the noise power, h_i denotes each interference fading gain and r_i is the distance from the interferer i to the typical receiver. Considering the most common interferences in the MAC layer performance evaluations, we assume a distance-dependent path-loss with an exponent. This straightforward model facilitates derivation of tractable closed-form expressions for both the transmission probability and the throughput.

Average successful content delivery probability: This is defined as the successful response to the typical receiver's file request when the requested file is successfully downloaded. The successful content delivery probability of a requested file defined as the probability that a receiver succeeds in decoding the received content from its associated transmitter. Thus when the typical receiver requests the j-th file from its serving node, given the received SINR, and the SINR target Θ_j, the success content delivery probability is expressed as

$$\mathcal{P}_{\mathrm{suc}}^j(\Theta_j) = p\left[\frac{P_m G_l |h_l|^2 {r_l}^{-\alpha_m}}{\sigma^2 + I_j} \ge \Theta_j\right], \tag{7}$$

where I_j is the interference received by the typical receiver given as

$$I_j = \underbrace{\sum_{i \in \Phi_j} P_m G_i |h_i|^2 r_i^{-\alpha_m}}_{I_{j-\mathrm{In}}} + \underbrace{\sum_{i \in \Phi_j^c} P_m G_i |h_i|^2 r_i^{-\alpha_m}}_{I_{j-\mathrm{Non}}}. \tag{8}$$

[5]We assume that the transmitter and its associated receiver have a perfect channel knowledge, and then adjust their steering orientation so as to achieve the maximum directionality gain.

By averaging over all file requests, the average successful content delivery probability is given as

$$\mathcal{P}_{\text{suc}}(\Theta) = \sum_{j=1}^{L} f_j \cdot \mathcal{P}^j_{\text{suc}}(\Theta_j), \tag{9}$$

where f_j is the probability of requesting the jth file.

Further, we present the analytical results in a couple of steps. In the first step, we illustrate the performance metrics without considering contention. Next, we characterize the performance metrics from the MAC layer perspective in the second step.

III. Cache Hit Ratio & Successful Content Delivery Probability

In this section, we characterize the cache hit ratio probabilities required for a cache-aided transmission in mmWave networks. To model the caching dynamics of a given node, we exploit the commonly used path loss distributions to derive the cache hit probability.

A. Cache hit characterization

We analyze the cache hit characterization in two cases corresponding to the two transmission mechanisms.

1) Nearest node: Denote $\mathcal{P}^n_h$ as the caching hit probability in the case of nearest node. Due to the probabilistic caching assumption, the probability of finding a file cached in a given area is strongly dependent on the blockages and the coverage area of the ad-hoc cell. Hence, the probability of finding a cache in the nearest transmitter node can be characterized with the nearest distance distribution which is illustrated in following lemma.

Lemma 1. *The nearest distance distribution for the case of LOS mmWave networks is given by*

$$F(r; q_j) = 1 - \exp\left(-\frac{2\pi q_j \lambda \left(1 - e^{-\beta\, r}(\beta\, r + 1)\right)}{\beta^2}\right). \tag{10}$$

Proof. The proof of this lemma is readily available in [47, Proposition 3]. However, for the sake of completeness we have also presented a sketch of the proof in Appendix A by leveraging some details from [47, Proposition 3]. □

Therefore, when a user requests a file j with a probability f_j and its caching probability is q_j, then the probability of finding that file in the nearest transmitter node is given by

$$\mathcal{P}^n_{h,j} = 1 - \exp\left(-\frac{2\pi q_j \lambda \left(1 - e^{-\beta\, r}(\beta\, r + 1)\right)}{\beta^2}\right). \tag{11}$$

Averaging over all the files, the cache hit probability is given as

$$\mathcal{P}^n_h = \sum_{i=1}^{L} f_j(1-q_j)\left(1 - \exp\left(-\frac{2\pi q_j \lambda \left(1 - e^{-\beta\, r}(\beta\, r + 1)\right)}{\beta^2}\right)\right). \tag{12}$$

Hence, we study the optimal caching probabilities for cache hit maximization. The optimization problem for maximizing the cache hit probability is given as

$$\begin{aligned} \mathbf{P1}: \max_{\mathbf{q}} \quad & \mathcal{P}^n_h \\ \text{s.t.} \quad & 0 \le q_j \le 1 \text{ for } j = 1, \cdots, L \\ & \sum_{j=1}^{L} q_j \le \mathcal{M} \end{aligned} \tag{13}$$

We observe that the second order derivative of P1 is strictly negative, thus $\mathcal{P}^n_h$ is a concave function for each j. Since the weighted sum of convex functions is also convex function, P1 is a constrained convex optimization problem. Thus a unique solution exists. Hence the Lagrangian function of P1 is given as

$$\mathcal{L}(q_j, \omega) = -1 + \sum_{j=1}^{L} f_j(1 - q_j) e^{-\frac{2\pi q_j \lambda \left(1 - e^{-\beta\, r}(\beta\, r + 1)\right)}{\beta^2}} + \omega\left(\sum_{i=1}^{L} q_j - \mathcal{M}\right), \tag{14}$$

where ω is the Lagrangian multiplier. This constrained optimization problem can be solved by applying the Karush-Kuhn-Tucker (KKT) conditions. Therefore, after differentiating $\mathcal{L}(q_j, \omega)$ with respect to q_j, we can obtain all the necessary KKT conditions. The optimal caching probabilities can be given as

$$q_j(\omega) = -\frac{\mathcal{W}(\frac{\omega}{q_j}\Xi)}{\Xi} + \frac{1}{\Xi} + 1, \tag{15}$$

where $\Xi = \frac{2\pi\lambda\left(-1 + e^{-\beta\, r}(\beta\, r + 1)\right)}{\beta^2}$ and $\mathcal{W}$ denotes the Lambert W function [48]. By applying the KKT condition again, we have

$$q^*_j(\omega) = \min\{[q_j(\omega^*)]^+, 1\}, \tag{16}$$

where $[x]^+ = \max\{x, 0\}$ and ω^* can be obtained by the Bisection method [29, Algorithm 1].

2) Best node: Taking into account the path loss of the mmWave LOS communication link, the minimum power received at the receiver is

$$\xi_l = P_m G_i\, r^{\alpha_{\text{L}}}. \tag{17}$$

Before advancing further, it is noted that (17) is important in the context of cache hit probability characterization. Also, the actual received signal power at the receiver may be reflected by the uncertainties like path loss, shadowing, and other fading factors, which causes a phenomenon commonly known as the ping-pong [49] effect. This outcome is avoided by using the long-term averaged power, which is determined by taking the mean of the received signal over a given period of time.

So, it is important to characterize such distributions in mmWave networks under the effect of blockages. As mentioned earlier in section II, any link *i.e.,* the distance between the receiver and transmitter in a mmWave network depends on the exponential blockage probability model. Therefore, the least pathloss distribution in a mmWave LOS network is not the same as for the case of a cellular network.

Lemma 2. *The least path loss distribution in a LOS mmWave network can be given as*

$$F_{\xi_l}(r;q_j)=1-\prod_{l,k\in\{\mathrm{M,m}\}}\exp\left(-\frac{2\pi\varsigma_{lk}q_j\lambda}{\beta^2}\times(1-e^{-\beta(rP_mG_i^{lk})^{\frac{1}{\alpha_L}}}(1+\beta(rP_mG_i^{lk})^{\frac{1}{\alpha_L}}))\right). \tag{18}$$

Proof. This proof follows from Lemma 1. □

Averaging over all the files, the cache hit probability is given as

$$\mathcal{P}_h^b=\sum_{i=1}^{L}f_i(1-q_j)F_{\xi_l}(r;q_j). \tag{19}$$

Hence, we study the optimal caching probabilities for cache hit maximization. The optimization problem for maximizing the cache hit probability is give as

$$\begin{aligned}\mathbf{P2}:\ \max_{\mathbf{q}}\quad & \mathcal{P}_h^b\\ \text{s.t.}\quad & 0\le q_j\le 1 \text{ for } j=1,\cdots,L\\ & \sum_{j=1}^{L}q_j\le\mathcal{M}\end{aligned} \tag{20}$$

The optimal solution of P2 can be solved by following similar approach in characterizing P1. Hence, for brevity, we have omitted the corresponding proof.

In next section, we characterize the average success probability from the perspective of the delivery phase. Particularly, the delivery phase involves communication policy, complicated fading channels, and interference. Therefore, for tractable analysis, the maximization of the average success probability hasn't been considered in this paper. Neverthless, it can be considered in future works.

B. Average Successful Content Delivery Probability

In the following proposition, we present the success probability at the typical receiver from a given mmWave transmitter for a predefined SINR threshold Θ_j.

Proposition 1. *The success probability of the SINR achieved at the typical receiver from a given mmWave transmitter node is given as*

$$\mathcal{P}_{suc}^j(\Theta_j;q_j(\omega))=\sum_{k=0}^{\nu}\binom{\nu}{k}(-1)^k\int_{y>0}e^{\frac{-Ak\Theta_j y\sigma^2}{P_mG_l}}\times\prod_{t\in\mathrm{L,N}}\mathbb{E}_{\mathcal{I}_{j-\mathrm{In}}^t}\left[e^{\frac{-Aky\Theta_j\mathcal{I}_{j-\mathrm{In}}^t}{P_mG_l}}\right]\mathbb{E}_{\mathcal{I}_{j-\mathrm{Non}}^t}\left[e^{\frac{-Aky\Theta_j\mathcal{I}_{j-\mathrm{Non}}^t}{P_mG_l}}\right]f_{\xi_l}(y)dy, \tag{21}$$

where ν is a parameter from the tight upper bound of Gamma distribution given as $\mathcal{P}[|h_l|^2<\gamma<(1-e^{-A\gamma})^\nu]$ with $A=\nu(\nu!)^{\frac{-1}{\nu}}$, f_ξ is the distribution of the least path loss which is the derivative of equation (18)*, and $\mathbb{E}_{\mathcal{I}_{j-\mathrm{In}}^t}[.]$ follows from Appendix B.*

Proof. See Appendix B. □

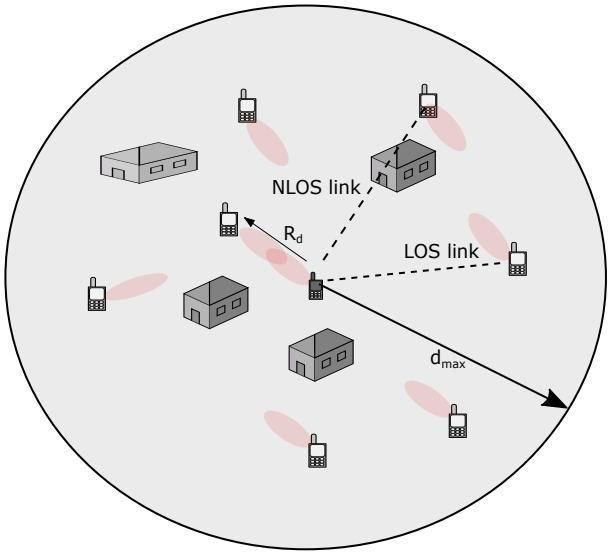

Fig. 2. Network model under contention protocol.

Consequently, the content average success probability maximized with $q_j^*(\omega)$ is given as

$$\mathcal{P}_{\mathrm{suc}}^*(\Theta)=\sum_{j=1}^{L}f_j\cdot\mathcal{P}_{\mathrm{suc}}^j(\Theta_j;q_j^*(\omega)). \tag{22}$$

IV. Contention Based Caching

In urban settings, the mmWave communications are prone to interference which can cause poor delivery rate to users. Moreover, the transmitters can create a significant interference to non-associated receivers in cache-aided transmissions. To tackle these issues, we leverage the benefits of using the MAC based contention protocol to mitigate the interference effect. Therefore, in this section, we investigate the transmission probability in a mmWave network considering the implementation with slotted ALOHA protocol. The derivation of such a result will play a major role in performance analysis of cache enabled MAC based mmWave networks.

A. Transmission Probability

In this section, we characterize the transmission probability of transmitter nodes in mmWave ad-hoc networks under the proposed contention based multimedia delivery protocol as described in Fig. 1 and Fig. 2.

Considering λ and ρ_a as the density of transmitters per unit area and the average probability of being active for every transmitter respectively, the nodes for which protocol condition (a), mentioned in Section II, follows a homogeneous PPP is defined as Φ^a with density λ^a. Therefore, the density of active transmitter nodes Φ^a under contention based protocol is $\lambda^a=\rho_a\lambda$.

It is worth noticing that the transmission probability also depends on the LOS case according to condition (b) in the proposed contention based multimedia delivery protocol. Hence, in the following lemma, we consider such an assumption. Let

$\mathcal{P}_d$ denote the probability that a transmitter node is under a request within the distance of R_d according to the condition (c). Hence we first derive $\mathcal{P}_d$ in the following lemma by following both conditions (b) and (c).

Lemma 3. *The probability that a transmitter node is under request in cache-enabled LOS mmWave ad-hoc networks is given as*

$$\mathcal{P}_d = \sum_{j=1}^{L} f_j (1-q_j) \left(1 - e^{\frac{2\pi q_j \lambda^a (1-e^{-\beta R_d(\beta R_d+1))}}{\beta^2}}\right). \quad (23)$$

Proof. This proof follows from Lemma 1. □

Let Φ^r be the point process formed by the active transmitter nodes over all file requests and let λ^r be the corresponding density.

Corollary 1. *For cache-enabled mmWave ad-hoc networks, the density of Φ^r under contention based protocol is given by*

$$\lambda^r = \mathcal{P}_d \lambda^a, \quad (24)$$

As the ad-hoc nodes are deployed randomly, the main lobe of the active transmitter coincides with the typical receiver having a probability of $\varsigma_{\mathrm{MM}} = (\frac{\theta}{2\pi})^2$. Consequently, the density of the aforementioned active transmitters under condition (d) are presented in the following corollary.

Corollary 2. *For cache-enabled mmWave ad-hoc networks, the density of Φ^r under condition (c) is given by*

$$\lambda^r = \varsigma_{\mathrm{MM}} \mathcal{P}_d \lambda^a, \quad (25)$$

Let Φ^r and Φ^{AL} denote the primary and the secondary point processes within the contention domain, respectively. Each transmitter competes with its neighboring nodes to access the shared wireless channel. The winning transmitters form Φ^{AL} process. Considering a generic transmitter $(x_i, m_i) \in \Phi^r$, we define $N(x_i)$ as the neighborhood contender set comprised of the nodes with contention threshold higher than $\mho$. It is observed for a symmetric channel gain that if a node is in the neighborhood set of x_i, then vice-versa also holds true. For the communication range $d_{\max}$ (by following condition (e)), the transmitter is allowed to transmit if and only if it has the lowest back-off timer among its neighborhood set of contenders $N(x_i)$. This lower limit is determined by dynamic alteration in the random-shape region, which is defined by the instantaneous path gain within the aforementioned communication range of $d_{\max}$.

The neighborhood set is determined by bounding the observation region by $\mathcal{B}_{x_i}(d_{\max})$, where $d_{\max}$ is a sufficiently large distance, such that the probability for a transmitter located beyond $d_{\max}$ to become a neighbor of x_i is a very small number, ϱ. Hence,

$$\mathcal{P}\left\{\frac{P_m G_l^{\max} H_m}{||x_i - x_j||^{\alpha}} > \mho \,|\, ||x_i - x_j|| > d_{\max}\right\} \leq \varrho. \quad (26)$$

Therefore, $d_{\max}$ can be deterministically computed as

$$d_{\max} = \left(\frac{P_m G_l^{\max}}{\mho} F_{H_m}^{-1}(\varrho)\right)^{1/\alpha}, \quad (27)$$

where, F^{-1} denotes the inverse of the CDF of H_m. Then the neighborhood success probability within the bounded region can be defined as

$$\mathcal{P}_\zeta = \mathcal{P}\{\gamma_{x_i,x_j} \geq \mho | x_j \in \mathcal{B}_{x_i}(d_{\max})\}. \quad (28)$$

Considering the blockages, (28) can be re-written as

$$\mathcal{P}_\zeta = \sum_{j\in \mathrm{L,N}} \int_0^{d_{\max}} \left(1 - F_{H_m}\left(\frac{\mho r^{\alpha_j}}{P_m (G_l^{\max})^2}\right)\right) p_j(r)\, r \mathrm{d}r,$$
$$= \sum_{j\in \mathrm{L,N}} \int_0^{d_{\max}} \left[\gamma\left(m, \frac{(\mho r^{\alpha_j})}{P_m G_l^{\max}}\right)\right] p_j(r)\, r \mathrm{d}r. \quad (29)$$

where, $\gamma(\cdot,\cdot)$ is the lower incomplete gamma function. A closed-form expression for $\mathcal{P}_\zeta$ can be computed numerically.

Therefore, based on Corollaries 1 and 2, and from (27) and (29), it is clear that we can advance towards the evaluation of the transmission probability of transmitters under the proposed contention based multimedia delivery protocol condition (f). To proceed, we leverage the results from [50] and incorporate additional blockage effects, as proposed in the following Lemma.

Lemma 4. *Assume that in the disc N, the transmission probability of a transmitter under the contention delivery protocol is $\mathcal{P}_d^{\mathrm{AL}} = \frac{1-e^{-N\mathcal{P}_\zeta}}{N\mathcal{P}_\zeta}$. Then the intensity of active number of transmitters is given by $\lambda^{\mathrm{AL}} = \lambda^r \mathcal{P}_d^{\mathrm{AL}}$ [50, Theorem 4.1].*

Proof. A generic transmitter in Φ^r is allowed to transmit in Φ^{AL} if and only if it has the lowest mark in its neighborhood set $N(x_i)$. If x_i has n neighbors, due to the uniform distribution of the marks among the neighbors of x_i, the probability that x_i has the lowest mark is $1/(n+1)$. Let us denote P_k as the probability of having k points in vicinity of $\mathcal{B}_{x_i}(d_{\max})$. Therefore, the number of points can be obtained by using the Corollary 3, expressed as follows

$$P_k = \frac{e^{-\lambda_j^r \pi d_{\max}^2} (\lambda_j^r \pi d_{\max}^2)^k}{k!}. \quad (30)$$

Averaging over both spatial and channel gain statistics, we have

$$\mathcal{P}_d^{\mathrm{AL}} = \mathrm{P}\{x_i \text{ is allowed to transmit in } \Phi^{\mathrm{AL}}\}, \quad (31)$$
$$= \sum_{n=0}^{\infty} \frac{1}{n+1} \sum_{k=n}^{\infty} P_k \binom{k}{n} (\mathcal{P}_\zeta)^n (1-\mathcal{P}_\zeta)^{k-1},$$
$$= \frac{e^{-\mathcal{N}}}{\mathcal{N}\mathcal{P}_\zeta} \sum_{n=0}^{\infty} \frac{(\mathcal{N}\mathcal{P}_\zeta)^{n+1}}{(n+1)!} \sum_{p=0}^{\infty} \frac{(\mathcal{N}(1-\mathcal{P}_\zeta))^p}{p!},$$
$$= \frac{1 - e^{-\mathcal{N}\mathcal{P}_\zeta}}{\mathcal{N}\mathcal{P}_\zeta},$$

where $p = k - n$ and $\mathcal{N} = \pi \lambda^r d_{\max}^2$.

□

Depending on the blockages and deployment constraints, we assume that the distribution of transmitters, Φ^{AL}, follows a contour according to its transmission probability. Correspondingly, it is clear that this distribution of the transmitter nodes is not spatially uniform, which can be clearly distinguished from

random and uniformly distributed network assumptions that lead to a Poison number of nodes per unit area $i.e.$, the PPP model. This model is widely adopted in the current literature [51]–[53]. The characterization of non-PPP models in general topologies using the Laplace Function and the probability generating functions is a challenging problem. Therefore, these thinned point processes are quite difficult to investigate as their probability generating functionals do not exist [54]–[56]. Hence, we adopt some approximations to introduce analytical tractability and assume that the nodes are distributed according to the PPP model. The density of these nodes is approximated by that of a thinned PPP with density λ^{AL}.

Assumption 3: The distribution of transmitters storing the file content j follows a PPP Φ_j^{AL} with density $q_j\lambda^{\mathrm{AL}}$. Similarly, the distribution of transmitters that do not store the file content j follows a PPP $\Phi_j^{\mathrm{AL-C}}$ with density $(1-q_j)\lambda^{\mathrm{AL}}$.

Before proceeding further, it is worthwhile to mention about the cache hit probabilities required for a cache aided transmission in MAC based mmWave networks. Under the PPP assumption, the cache hit probabilities are exactly the same as in equations (10) and (18) with $q_j\lambda^{\mathrm{AL}}$.

B. Average Successful Content Delivery Probability

By possession of cache hit placement vector $\mathbf{q}$ and transmission probability, we are ready to characterize the average success probability of a typical transmission under MAC based protocol. In this turn, leveraging from Proposition 1, the average success probability for content delivery is the same as equation (21) with the PPP approximated density λ^{AL}.

Corollary 3. *The average success probability of content delivery at the typical receiver from a given mmWave transmitter node under MAC based protocol is given in equation* (21) *with* λ^{AL}.

Special case: For a generalized analysis, we give a bound on the average success probability of content delivery without considering PPP assumption in following Proposition.

Proposition 2. *The success probability of the content delivery at the typical receiver from a given mmWave transmitter node under contention based protocol is given as:*

$$\mathcal{P}_{suc}^{j}(\Theta_j)=\sum_{k=0}^{\nu}\binom{\nu}{k}(-1)^k e^{\frac{-A\,k\,\Theta_j R_d^{-\alpha_{\mathrm{L}}}\sigma^2}{P_m G_l}} \tag{32}$$
$$\times\prod_{t\in\mathrm{L,N}}\mathbb{E}_{\mathcal{I}_{j-\mathrm{In}}^t}\left[e^{\frac{-AkR_d^{-\alpha_{\mathrm{L}}}\Theta_j\mathcal{I}_{j-\mathrm{In}}^t}{P_m G_l}}\right]\mathbb{E}_{\mathcal{I}_{j-\mathrm{Non}}^t}\left[e^{\frac{-A\,k\,R_d^{-\alpha_{\mathrm{L}}}\Theta_j\mathcal{I}_{j-\mathrm{Non}}^t}{P_m G_l}}\right],$$

where

$$\mathbb{E}_{\mathcal{I}_{j-\mathrm{In}}^t}\left[\exp\left(\frac{-A\,k\,R_d^{-\alpha_{\mathrm{L}}}\Theta_j\mathcal{I}_{j-\mathrm{In}}^t}{P_m G_l}\right)\right]=e^{\Xi_{j-\mathrm{In}}^t}, \tag{33}$$

where

$$\Xi_{j-\mathrm{In}}^t=\sum_{l,k\in\{\mathrm{M,m}\}}\nu\,\varsigma_{lk}\left(\pi\left(\bar{s}\right)^{-1/\alpha_t}\csc\left(\frac{\pi}{\alpha_t}\right)\right. \tag{34}$$
$$+\frac{(\alpha_t-1)d_{\max}^{\alpha_t}\log\left(\bar{s}d_{\max}^{-\alpha_t}+1\right)}{\alpha_t-1}$$
$$\left.-\frac{d_{\max}^{1-\alpha_t}\left(\alpha_t\bar{s}\,{}_2F_1\left(1,\frac{\alpha_t-1}{\alpha_t};2-\frac{1}{\alpha_t};-d_{\max}^{-\alpha_t}\bar{s}\right)\right)}{\alpha_t-1}\right),$$

$\bar{s}=\frac{s\,P_m G_i^{lk}}{\nu}$, $s=\frac{-A\,k\,R_d^{-\alpha_{\mathrm{L}}}\Theta_j}{P_m G_l}$ *and* ${}_2F_1$ *is the Hypogeometric function.*

Proof. Refer Appendix C. □

V. Numerical Analysis

In this section, we validate our system model and also verify the accuracy of the derived analytical results. In general, the computations are performed through Monte Carlo simulations, which are then used to validate the analytical results. Unless stated otherwise, most of the values of the parameters used are inspired from literature mentioned in the references [8], [11]. A few of the parameters and their corresponding values are given in Table I. All other parameters and values will be explicitly mentioned wherever used.

First, we compare the cache hit probability with different node selections and for various blockage densities. These results demonstrate lemmas 1 and 2. Fig. 3 depicts the analytical results for the variation in the cache hit probability with increasing density of ad-hoc nodes (λ). Clear distinction between the random file caching where the files are cached in the ad-hoc nodes at random, and optimal file caching where the files are cached with more diversity in the ad-hoc nodes is presented for the nearest and best selection criterion. In the nearest selection, the ad-hoc node closest to the typical receiver is selected while in the best selection, an ad-hoc node is chosen based on the largest channel gain. It is seen that the cache-hit probability increases with the increase in number of ad-hoc nodes, which is obvious as the probability of storing the files becomes high with increase in the ad-hoc nodes.

TABLE II
Simulation Parameters

Notation	Parameter	Values
R_d	Radius of the nearest node	75 meters
$d_{\max}$	Radius of the bounded region	250 meters
λ	Density of ad-hoc nodes	0.0005
β	Blockage density	0.0143
G^M	Antenna gain of main lobe	10 dB
G^m	Antenna gain of side lobe	0 dB
$\alpha_{\mathrm{L}},\alpha_{\mathrm{N}}$	Path loss exponent	LOS-2.1, NLOS-3.5
P_{S}	Node transmit power	1 Watt
$\eth$	Contention threshold	10 dB
N_0	Noise power	Thermal noise + 10dB noise figure.
L	No of files	5
M	Cache size	3
γ	Zipf exponent	1.4

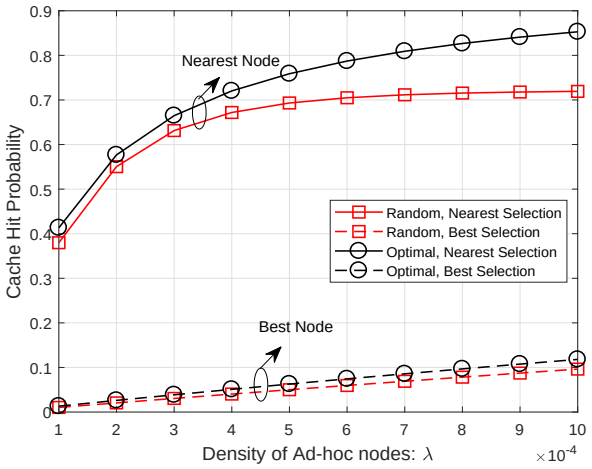

Fig. 3. The Cache Hit Probability versus Density of Ad-hoc Nodes (λ) $[\times 10^{-4}]$ for different criterion with random and optimal selections of file caching.

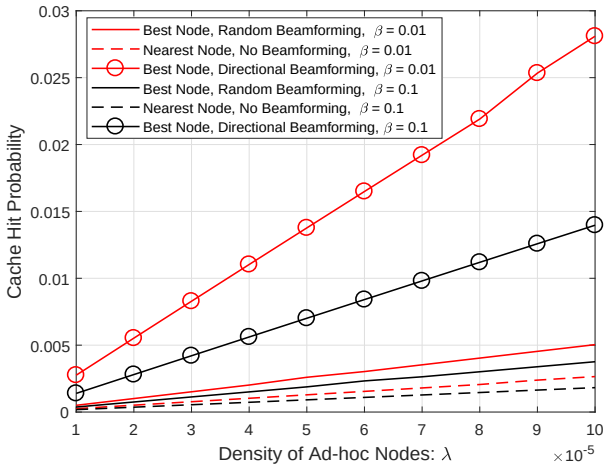

Fig. 4. The Cache Hit Probability versus Density of Ad-hoc Nodes (λ) for different selection criterion among the best and nearest nodes considering random, none, and directional beamforming methods.

Moreover, the random file and optimal file caching techniques are compared in this figure. It is clear from the figure that the optimal caching technique outperforms the random file caching technique.

Fig. 4 illustrates the transition in the values of cache hit probability with increasing density of ad-hoc nodes (λ) for different values of blockage density (β). Same as in Fig. 3, a divergence analysis is illustrated for the best and nearest ad-hoc node selections but implementing the random, no, and directional beamforming methods. It is seen that the cache hit probability decreases with increasing values of β. However as expected, the results of directional beamforming method with proper beam alignment between the transmitter and receiver outperforms both the no beamforming method with omni-directional radiation and random beamforming method with non-alignment of beams. Additionally, it is observed that the random beamforming method performs better than the no beamforming method for decreasing β. It is also seen that the blockages have an adverse effect on cache hit probability.

Fig. 5 presents the plot of the cache hit probability against the order of files for various selections of caching size (M) and Zipf coefficient (γ). It is found that the cache hit probability increases with the increasing M and γ values. However, the cache hit probability declines considerably according to the parameter value selections of M and γ as the order of files within the ad-hoc node increases.

After establishing the effect of cache hit probability in the previous figures, we now look into the average successful delivery probability. Hence, Fig. 6 shows the plot of the average success probability of content delivery versus SINR threshold (in dB) for various values of Caching size (M) and Zipf coefficient (γ). As mentioned earlier, the average successful content delivery probability increases with increas-

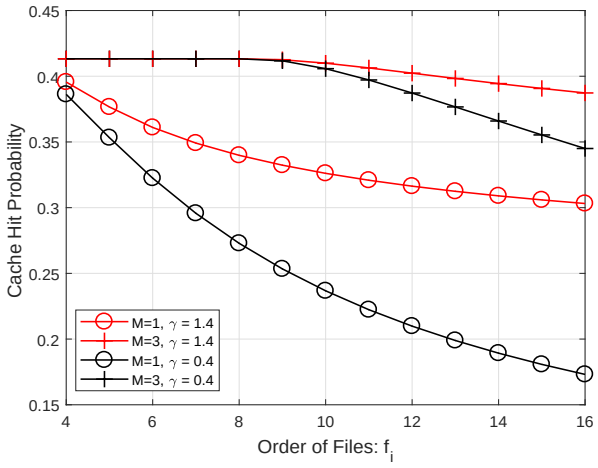

Fig. 5. The Cache Hit Probability versus Order of files (f_i) for different parameter values of Caching size (M) and Zipf coefficient (γ).

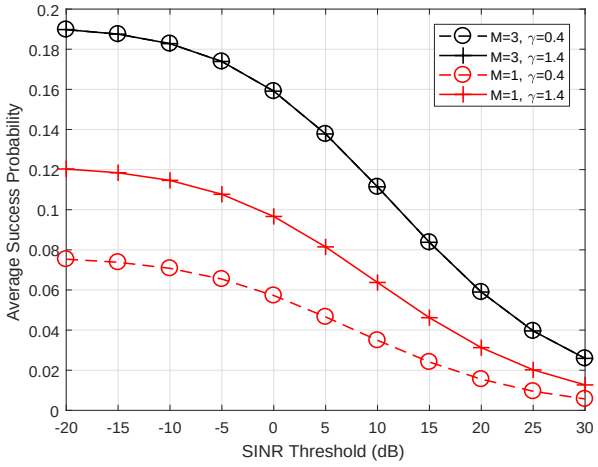

Fig. 6. Average success probability of content delivery versus SINR threshold [in dB] for various values of Caching size (M) and Zipf coefficient (γ).

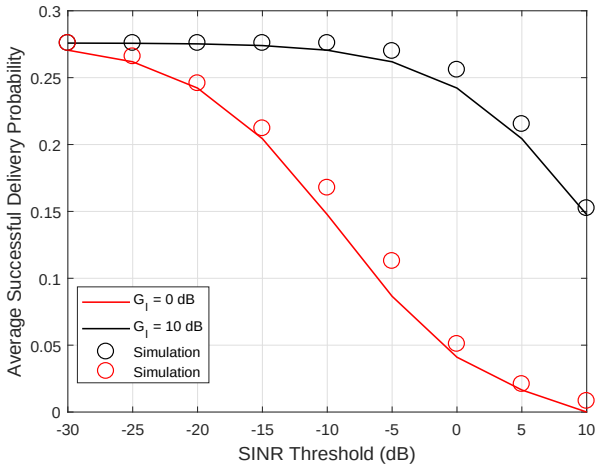

Fig. 7. Average success probability of content delivery versus SINR threshold [in dB] for various values of antenna gain values at the receiver considering ideal and proposed cases.

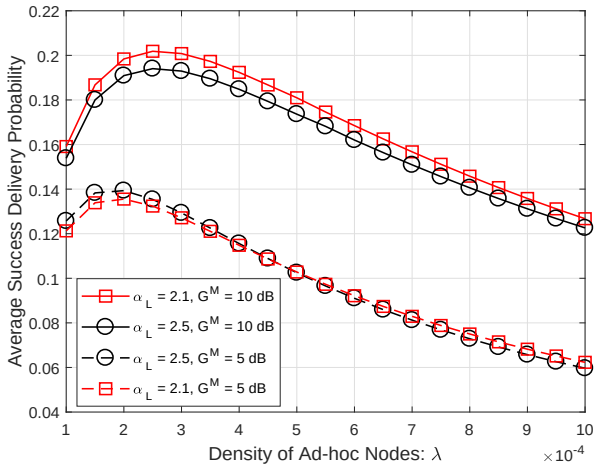

Fig. 9. Average successful delivery probability versus SINR threshold [in dB], comparing the proposed system with MAC protocol and the one without MAC protocol.

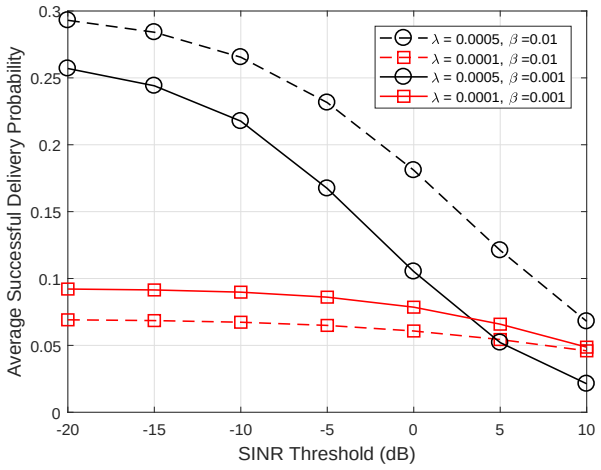

Fig. 8. Average success probability of content delivery versus SINR threshold [in dB] for different values of conditional distribution of potential interferers (λ) and density of blockage in the network (β).

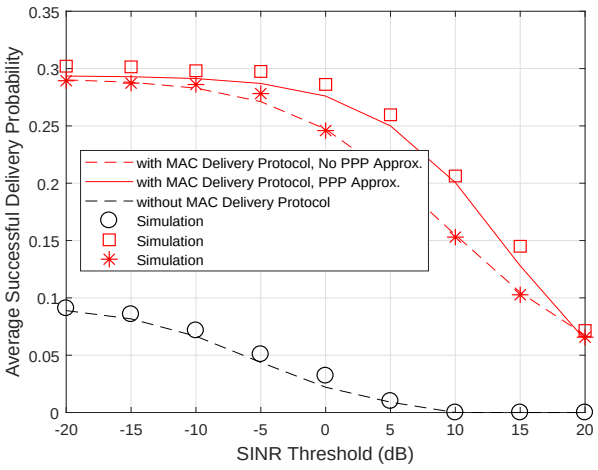

Fig. 10. Average success probability of content delivery versus SINR threshold [in dB] comparing the proposed system with MAC protocol and the one without MAC protocol.

ing M and γ values. The same is found to hold true in this case. Nevertheless, it is illustrated in Fig. 6 that the average success probability of content delivery decreases significantly with increasing SINR threshold values.

Fig. 7 highlights the average success probability of content delivery versus SINR threshold (in dB) for different values of antenna gain values at the receiver. It is found that the average success probability of content delivery increases with increasing antenna gain values at the receiver. This is due to the fact that the larger antenna gains mitigate the effects of path loss in communication. Therefore, the delivery rate increases with respect to antenna gains. As expected, it is observed that the average successful delivery probability decreases considerably with increasing SINR threshold values.

Fig. 8 represents the plot of average success probability of content delivery against SINR threshold for different parameter values of density of nodes (λ) and density of blockage in the network (β). It is seen that the average success probability of content delivery decreases with increasing SINR threshold values. Interestingly, it is observed that the effect of density of blockage in the network (β) is minimal in the case of low interferers as depicted in the red curves. However, vice-versa holds true in the case with high potential interferers as shown in the black curves. This reverse effect is helpful in determining how more blockages are beneficial in the case with more interferers' density as the average success probability of content delivery increases significantly. In addition, it is noteworthy that the average success probability of content delivery increases as the density of ad-hoc nodes increases. However, the increasing density does not always favor the average success probability of content delivery as it introduces higher interference in the network. We explain such phenomena in next figure.

In conjunction with previous Fig. 8 and Fig. 9 plots the

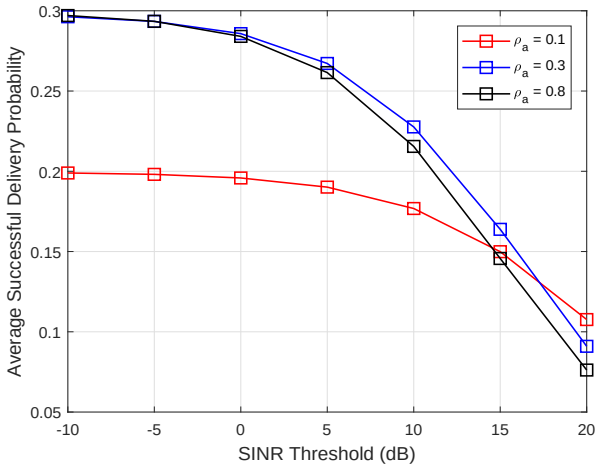

Fig. 11. Average successful delivery probability versus SINR threshold [in dB] for various ρ_a with MAC protocol.

average success probability of content delivery as a function node density for various path-loss exponents. It is clear from the figure that the LOS path loss exponent has minor effect on the the average success probability. It can be explained from the fact that the mmWave LOS channel is less likely change due to channel conditions. It is worthy of mention that there is an optimal value of the average success probability of content delivery as indicated by the shape of the curves in Fig. 9 with the implication that increasing the ad-hoc node density has a diminishing returns effect. Analytical determination of this optimal point can be explored in future works.

Fig. 10 depicts the plot of average success probability of content delivery against SINR threshold comparing the proposed system with MAC protocol and the one without MAC protocol. As explained in section IV. B, the average success probability of content delivery is derived for two cases, i.e., by considering PPP approximation of ad-hoc nodes in Corollary 3 and without PPP approximation in Proposition 2. Hence, one could see the tightness of both the cases in figures. It is also seen that average success probability decreases as the SINR threshold decreases for both the cases. The proposed system with mmWave and MAC protocol outperforms the one without MAC protocol. It is needless to mention that the proposed protocol reduces the number of concurrent transmissions, thereby leading to a higher successful probability of content delivery.

Fig. 11 represents the plot of average success probability of content delivery against SINR threshold for different parameter values of ρ_a. The average successful delivery probability is found to be decreasing with increasing values of SINR, as expected. One can intuitively assume that the average success delivery probability should increase with increasing ρ_a values. However, it is observed that the average success probability of successful delivery increases for a fixed SINR until a certain value of ρ_a, implying a fixed upper bound for the low SINR values. Thereafter, increasing the probability of transmission ρ_a does not always favor the average successful delivery probability due to the introduction of high interference in the network.

VI. Conclusion

The potential benefits of deploying cache-enabled ad-hoc nodes in outdoor mmWave networks were investigated. Moreover, we characterize the optimal caching placement with respect to blockages in the mmWave network. Then, we evaluate the performance of the proposed caching placement algorithm and compare it with two different caching strategies: 1) nearest node, and 2) best node placement. From our analysis, it is clear that the cache hit probability depends on the blockage density and network conditions such as path loss exponent, antenna gain, and density of the ad-hoc nodes. Accordingly, the average successful content delivery probability for the ad-hoc nodes was studied. Since interference increases with the number of nodes, a trade-off can be observed between the cache hit probability and the content delivery probability with respect to the density of nodes. Hence, a carefully designed MAC based protocol has been taken into consideration. Consequently, the average successful content delivery probability for the ad-hoc nodes based on the bounded region was studied.

The current work focuses on the ad-hoc networks only. However, it provides a cornerstone and importantly, the essential understanding for development of future cache-enabled cellular networks. In future, we will consider machine learning based approaches to learn the popularity of contents.

Appendix A
Proof of Lemma 1

Consider a Poisson point process, where the separation between the points represent the distance between the corresponding receiver and randomly placed transmitters in a mmWave network. Let us denote $\phi = \left\{\zeta \triangleq x\right\}$ as a homogeneous PPP with intensity λ. Here, the distance is to be considered as a random variable, and that its LOS state occurs with the probability of $e^{-\beta x}$. By using the Mapping theorem [57, Theorem 2.34], the density function of this one dimensional PPP under the effect of blockages can be given by

$$\Lambda([0,z]) = \int_0^z 2\pi\lambda x e^{-\beta x}\mathrm{dx}. \tag{35}$$

Using the void probability of a PPP and with the help of (35), the nearest node distribution in a mmWave network can be computed accordingly. Hence, this concludes the proof.

Appendix B
Proof of Proposition 1

The average success probability conditioned on the least path loss from the best node to the typical receiver is defined as

$$\mathcal{P}^j_{\text{suc}}(\Theta_j) = \int_{y>0} \mathcal{P}\left[\frac{P_m G_l |h_l|^2 y}{\sigma^2 + I_j} > \Theta_j\right] f_{\xi_l}(y)\,\mathrm{dy}.$$

Given that the small scale fading $\{h_l\}$, follows the Nakagami distribution, and employs the upper bound

of gamma distribution with a parameter ν such that $\mathcal{P}\left[|h_l|^2 < \gamma < (1-e^{-A\gamma})^{\nu}\right]$ with $A = \nu(\nu!)^{\frac{-1}{\nu}}$, therefore, the average success probability is expressed as:

$$\mathcal{P}\left[\frac{P_m G_l |h_l|^2 y}{\sigma^2 + I_j} > \Theta_j\right] = \sum_{k=0}^{\nu} \binom{\nu}{k} (-1)^k e^{\frac{-A\,k\,y\Theta_j\,\sigma^2}{P_m\,G_l}} \times \prod_{t\in \mathrm{L,N}} \mathbb{E}_{\mathcal{I}^t_{j-\mathrm{In}}}\left[e^{\frac{-A\,k\,y\Theta_j\,\mathcal{I}^t_j}{P_m\,G_l}}\right] \mathbb{E}_{\mathcal{I}^t_{j-\mathrm{Non}}}\left[e^{\frac{-A\,k\,y\Theta_j\,\mathcal{I}^t_j}{P_m\,G_l}}\right], \tag{36}$$

which follows from applying binomial expansion, and due to the fact that interference links can be LOS or NLOS such that $\mathcal{I}_j = \mathcal{I}^{\mathrm{L}}_{j-\mathrm{In}} + \mathcal{I}^{\mathrm{N}}_{j-\mathrm{Non}}$.

Hence the expectation of the LOS interfering link is given as:

$$\mathbb{E}_{\mathcal{I}^{\mathrm{L}}_{j-\mathrm{In}}}\left[\exp\left(\frac{-A\,k\,y\,\Theta_j\,\mathcal{I}^{\mathrm{L}}_{j-\mathrm{In}}}{P_m G_l}\right)\right] = \mathbb{E}_{\mathcal{I}^{\mathrm{L}}_{j-\mathrm{In}}}\left[\prod_{i\in\Phi_j^c} \exp\left(\frac{-A\,k\,y\,\Theta_j\,G_i\,|h_i|^2}{P_m G_l\, r_i^{\alpha_{\mathrm{L}}}}\right)\right], \tag{37}$$

gotten by substituting $\mathcal{I}^{\mathrm{L}}_{j-\mathrm{In}} = \sum_{i\in\Phi_j^c} P_m G_i |h_i|^2 r^{-\alpha_{\mathrm{L}}}$. Applying the probability generating functional of PPP (PGFL) [41], we obtain

$$\mathbb{E}_{\mathcal{I}^{\mathrm{L}}_{j-\mathrm{In}}}\left[\exp\left(\frac{-A\,k\,y\,\Theta_j\,\mathcal{I}^{\mathrm{L}}_{j-\mathrm{In}}}{P_m G_l}\right)\right] = \prod_{l,k\in\{\mathrm{M,m}\}} \exp\left(-2\,\pi \times \varsigma_{lk} q_j \lambda \int_0^{\infty}\left(1 - \frac{1}{\left(1+\frac{A\,k\,G_i^{lk}\,\Theta_j\,y}{P_m G_l\, r^{\alpha_{\mathrm{L}}}}\right)^{\nu}} p_{\mathrm{L}}(r)\mathrm{d}r\right)\right). \tag{38}$$

The expectation of NLOS interfering link can be obtained similarly.

Appendix C
Proof of Proposition 2

The average success probability conditioned on LOS within radius of R_d is given as

$$\mathcal{P}\left[\frac{P_m G_l |h_l|^2 R_d^{-\alpha_{\mathrm{L}}}}{\sigma^2 + I_j} > \Theta_j\right] = \sum_{k=0}^{\nu}\binom{\nu}{k}(-1)^k e^{\frac{-A\,k\,R_d^{-\alpha_{\mathrm{L}}}\Theta_j\,\sigma^2}{P_m\,G_l}} \times p_{\mathrm{L}}(R_d) \prod_{t\in\mathrm{L,N}} \mathbb{E}_{\mathcal{I}^t_{j-\mathrm{In}}}\left[e^{\frac{-A\,k\,R_d^{-\alpha_{\mathrm{L}}}\Theta_j\,\mathcal{I}^t_j}{P_m\,G_l}}\right] \mathbb{E}_{\mathcal{I}^t_{j-\mathrm{Non}}}\left[e^{\frac{-A\,k\,R_d^{-\alpha_{\mathrm{L}}}\Theta_j\,\mathcal{I}^t_j}{P_m\,G_l}}\right], \tag{39}$$

Hence the expectation of the LOS interfering link is given as

$$\mathbb{E}_{\mathcal{I}^{\mathrm{L}}_{j-\mathrm{In}}}\left[\exp\left(\frac{-A\,k\,R_d^{-\alpha_{\mathrm{L}}}\Theta_j\,\mathcal{I}^{\mathrm{L}}_{j-\mathrm{In}}}{P_m G_l}\right)\right] = \mathbb{E}_{\mathcal{I}^{\mathrm{L}}_{j-\mathrm{In}}}\left[\prod_{i\in\Phi_j^{\mathrm{AL}}} \exp\left(\frac{-A\,k\,R_d^{-\alpha_{\mathrm{L}}}\,\Theta_j\,G_i\,P_m|h_i|^2}{P_m G_l\, r_i^{\alpha_{\mathrm{L}}}}\right)\right], \tag{40}$$

gotten by substituting $\mathcal{I}^{\mathrm{L}}_{j-\mathrm{In}} = \sum_{i\in\Phi_j^{\mathrm{AL}}} P_m G_i |h_i|^2 r^{-\alpha_{\mathrm{L}}}$.

For the case of PPP, the closed-form/intergral expression for interference can be computed by applying the PGFL. However, the transmitter nodes in contention domain does not hold PPP assumption anymore. Therefore, by denoting $s = \frac{-A\,k\,R_d^2\,\Theta_j}{P_m G_l}$, we have

$$\begin{aligned}
&\mathbb{E}_{\mathcal{I}^{\mathrm{L}}_{j-\mathrm{In}}}\left[\exp\left(s\mathcal{I}^{\mathrm{L}}_{j-\mathrm{In}}\right)\right] \\
&= \mathbb{E}_{\Phi^{\mathrm{AL}},G_i,h_i}\left[\exp\left(-s\,P_m G_i h_i ||r_i||^{-\alpha_{\mathrm{L}}}\right)\right], \\
&\overset{(a)}{=} \mathbb{E}_{\Phi_j^{\mathrm{AL}},G_i}\left\{\prod_{i\in\Phi_j^{\mathrm{AL}}} \mathbb{E}_{h_i}\left[\exp\left(-s\,P_m G_i h_i ||r_i||^{-\alpha_{\mathrm{L}}}\right)\right]\right\}, \\
&\overset{(b)}{=} \mathbb{E}_{\Phi_j^{\mathrm{AL}},G_i}\left\{\prod_{i\in\Phi_j^{\mathrm{AL}}}\left(\frac{1}{1+\frac{s\,P_m G_i}{\nu} r^{-\alpha_{\mathrm{L}}}}\right)^{\nu}\right\}, \\
&= \mathbb{E}_{\Phi^{\mathrm{AL}},G_i}\left\{e^{-\sum\limits_{i\in\Phi_j^{\mathrm{AL}}}\log\left(\frac{1}{1+\frac{s\,P_m G_i}{\nu} r^{-\alpha_{\mathrm{L}}}}\right)^{\nu}}\right\}, \\
&\overset{(c)}{>} e^{\mathbb{E}_{\Phi_j^{\mathrm{AL}},G_i}\left\{-\sum\limits_{i\in\Phi_j^{\mathrm{AL}}}\log\left(\frac{1}{1+\frac{s\,P_m G_i}{\nu} r^{-\alpha_{\mathrm{L}}}}\right)^{\nu}\right\}},
\end{aligned} \tag{41}$$

$$\tag{42}$$

where (a) follows from the assumption of independent small scale fading, (b) follows from the use of the moment generating function of Nakagami-m random variable and (c) follows due to the use of Jensen's inequality.

Let,

$$\Xi = \mathbb{E}_{\Phi_j^{\mathrm{AL}},G_i}\left\{-\sum_{i\in\Phi_j^{\mathrm{AL}}}\Delta_i(r)\right\}, \tag{43}$$

where

$$\Delta_i(r) = \log\left(\frac{1}{1+\frac{s\,P_m G_i}{\nu} r^{-\alpha_{\mathrm{L}}}}\right)^{\nu}. \tag{44}$$

Therefore, using Campbell's theorem on point process, we have

$$\begin{aligned}
\Xi &= \sum_{l,k\in\{\mathrm{M,m}\}} \nu\,\varsigma_{lk} \int_0^{d_{\max}} \lambda_j^{\mathrm{AL}} \log\left(1+\bar{s} r^{-\alpha_{\mathrm{L}}}\right)\mathrm{d}r, \\
&= \sum_{l,k\in\{\mathrm{M,m}\}} \nu\,\varsigma_{lk}\left(\pi\,(\bar{s})^{-1/\alpha_{\mathrm{L}}}\csc\left(\frac{\pi}{\alpha_{\mathrm{L}}}\right)\right. \\
&\quad + \frac{(\alpha_{\mathrm{L}}-1) d_{\max}^{\alpha_{\mathrm{L}}} \log\left(\bar{s} d_{\max}^{-\alpha_{\mathrm{L}}}+1\right)}{\alpha_{\mathrm{L}}-1} \\
&\quad \left. - \frac{d_{\max}^{1-\alpha_{\mathrm{L}}}\left(\alpha_{\mathrm{L}}\bar{s}\,{}_2F_1\left(1, \frac{\alpha_{\mathrm{L}}-1}{\alpha_{\mathrm{L}}}; 2-\frac{1}{\alpha_{\mathrm{L}}}; -d_{\max}^{-\alpha_{\mathrm{L}}}\bar{s}\right)\right)}{\alpha_{\mathrm{L}}-1}\right),
\end{aligned} \tag{45}$$

where $\bar{s} = \frac{s\,P_m G_i^{lk}}{m}$ and ${}_2F_1$ is the Hypogeometric function.

References

[1] C. V. Mobile, "Cisco visual networking index: global mobile data traffic forecast update, 2011–2016," *San Jose, CA*, vol. 1, 2016.

[2] D. Tse and P. Viswanath, *Fundamentals of wireless communication*. Cambridge university press, 2005.

[3] K. Shanmugam, N. Golrezaei, A. G. Dimakis, A. F. Molisch, and G. Caire, "Femto caching: Wireless content delivery through distributed caching helpers," vol. 59, pp. 8402–8413, 2013.

[4] M. Ji, G. Caire, and A. F. Molisch, "Fundamental limits of caching in wireless D2D networks," *IEEE Trans. on Inf. Theory*, vol. 62, pp. 849 – 869, 2016.

[5] R. A. Stern and R. W. Babbitt, "Millimeter wave microstrip circulator," Jun. 7 1988, US Patent 4,749,966.

[6] R. C. Daniels, J. N. Murdock, T. S. Rappaport, and R. W. Heath, "60 GHz wireless: Up close and personal," *IEEE Microw. Mag.*, vol. 11, no. 7, pp. 44–50, 2010.

[7] O. El Ayach, S. Rajagopal, S. Abu-Surra, Z. Pi, and R. W. Heath, "Spatially sparse precoding in millimeter wave MIMO systems," *IEEE Trans. on Wireless Commun.*, vol. 13, no. 3, pp. 1499–1513, 2014.

[8] S. Singh, M. N. Kulkarni, A. Ghosh, and J. G. Andrews, "Tractable model for rate in self-backhauled millimeter wave cellular networks," *IEEE J. Select. Areas Commun.*, vol. 33, no. 1, pp. 2196–2211, Jan. 2015.

[9] M. N. Kulkarni, A. Alkhateeb, and J. G. Andrews, "A tractable model for per user rate in multiuser millimeter wave cellular networks," in *2015 49th Asilomar Conference on Signals, Systems and Computers*, Nov 2015, pp. 328–332.

[10] N. Bhushan, J. Li, D. Malladi, R. Gilmore, D. Brenner, A. Damnjanovic, R. T. Sukhavasi, C. Patel, and S. Geirhofer, "Network densification: the dominant theme for wireless evolution into 5G," *IEEE Commun. Mag.*, vol. 52, no. 2, pp. 82–89, 2014.

[11] A. Thornburg, T. Bai, and R. W. Heath, "Performance analysis of mmWave ad hoc networks," *IEEE Trans. Signal Process.*, vol. 64, no. 15, pp. 4065 – 4079, Apr. 2016.

[12] E. Turgut and M. C. Gursoy, "Coverage in heterogeneous downlink millimeter wave cellular networks," *IEEE Trans. on Commun.*, vol. 65, pp. 4463–4477, May 2017.

[13] J. Song, H. Song, and W. Choi, "Optimal caching placement of caching system with helpers," in *IEEE International Conference on Communications (ICC)*, June 2015, pp. 1825–1830.

[14] T. Kohonen, *Content-addressable memories*. Springer Science & Business Media, 2012, vol. 1.

[15] G. Ananthanarayanan, A. Ghodsi, A. Wang, D. Borthakur, S. Kandula, S. Shenker, and I. Stoica, "Pacman: coordinated memory caching for parallel jobs," in *Proceedings of the 9th USENIX conference on Networked Systems Design and Implementation*. USENIX Association, 2012, pp. 20–20.

[16] L. Zhang, M. Zhang, L. Fan, D. Wang, and P. Ienne, "Spontaneous reload cache: Mimicking a larger cache with minimal hardware requirement." in *NAS*, 2013, pp. 31–40.

[17] G. Paschos, E. Bastug, I. Land, G. Caire, and M. Debbah, "Wireless caching: Technical misconceptions and business barriers," *IEEE Commun. Magazine*, vol. 54, no. 8, pp. 16–22, 2016.

[18] E. Bastug, M. Bennis, and M. Debbah, "Living on the edge: The role of proactive caching in 5G wireless networks," *IEEE Commun. Mag.*, vol. 52, no. 8, pp. 82–89, 2014.

[19] T. X. Vu, S. Chatzinotas, and B. Ottersten, "Coded caching and storage planning in heterogeneous networks," in *IEEE Conference on Wireless Communications and Networking (WCNC)*, San Francisco, CA, USA, Mar. 2017.

[20] ——, "Edge-caching wireless networks: Performance analysis and optimization," *IEEE Trans. Wireless Commun.*, vol. PP, no. 99, pp. –, 2018.

[21] L. Lei, L. You, G. Dai, T. X. Vu, D. Yuan, and S. Chatzinotas, "A deep learning approach for optimizing content delivering in cache-enabled hetnet," in *International Symposium on Wireless Communication Systems*, Bologna, Italy, 2017.

[22] T. X. Vu, L. Lei, S. Vuppala, S. Chatzinotas, and B. Ottersten, "Energy-efficient design for latency-tolerant content delivery networks," in *Proc. IEEE WCNC Workshop*, Barcelona, Spain, Apr. 2018, pp. 1–6.

[23] N. Golrezaei, P. Mansourifard, A. F. Molisch, and A. G. Dimakis, "Base-station assisted device-to-device communications for high-throughput wireless video networks," *IEEE Transactions on Wireless Communications*, vol. 13, pp. 3665–3676, 2014.

[24] E. Bastug, M. Bennis, and M. Debbah, "Living on the edge: The role of proactive caching in 5G wireless networks," *IEEE Communications Magazine*, vol. 52, pp. 82–89, 2014.

[25] M. Mitici, J. Goseling, M. de Graaf, and R. J. Boucherie, "Optimal deployment of caches in the plane," in *IEEE Global Conference on Signal and Information Processing (GlobalSIP)*, Dec 2013, pp. 863–866.

[26] S. T. ul Hassan, M. Bennis, P. H. J. Nardelli, and M. Latva-aho, "Caching in wireless small cell networks: A storage-bandwidth tradeoff," *IEEE Communications Letters*, vol. 20, no. 6, pp. 1175–1178, June 2016.

[27] C. Jarray and A. Giovanidis, "The effects of mobility on the hit performance of cached D2D networks," in *Proc. of International Symposium on Modeling and Optimization in Mobile, Ad Hoc, and Wireless Networks (WiOpt)*, Tempe, AZ, USA, May 2016.

[28] N. Golrezaei, P. Mansourifard, A. F. Molisch, and A. G. Dimakis, "Base-station assisted device-to-device communications for high-throughput wireless video networks," *IEEE Transactions on Wireless Communications*, vol. 13, no. 7, pp. 3665–3676, July 2014.

[29] S. H. Chae and W. Choi, "Caching placement in stochastic wireless caching helper networks: Channel selection diversity via caching," *IEEE Transactions on Wireless Communications*, vol. 15, no. 10, pp. 6626–6637, Oct 2016.

[30] D. Malak, M. Al-Shalash, and J. G. Andrews, "Optimizing the spatial content caching distribution for device-to-device communications," in *Proc. of IEEE International Symposium on Information Theory (ISIT)*, Barcelona, Spain, Aug. 2016.

[31] D. M. abd M. Al-Shalash and J. G. Andrews, "Optimizing content caching to maximize the density of successful receptions in device-to-device networking," *IEEE Transactions on Communications*, vol. 64, pp. 4365–4380, Oct. 2016.

[32] Z. Chen, N. Pappas, and M. Kountouris, "Probabilistic caching in wireless D2D networks: Cache hit optimal versus throughput optimal," *IEEE Communications Letters*, vol. 21, pp. 584–587, Nov. 2016.

[33] M. Ji, G. Caire, and A. F. Molisch, "D2D-aware device caching in mmwave-cellular networks," *IEEE J. Sel. Areas Commun.*, vol. 34, no. 1, pp. 176–189, Jan. 2016.

[34] N. Giatsoglou, K. Ntontin, E. Kartsakli, A. Antonopoulos, and C. Verikoukis, "D2D-aware device caching in mmWave-cellular networks," *IEEE J. Sel. Areas Commun.*, vol. 35, pp. 2025–2037, Jun. 2017.

[35] N. Deng, W. Zhou, and M. Haenggi, "The ginibre point process as a model for wireless networks with repulsion," *IEEE Transactions on Wireless Communications*, vol. 4, pp. 107–121, Jan. 2015.

[36] F. Zabini and A. Conti, "Ginibre sampling and signal reconstruction," in *Proc. of IEEE International Symposium on Information Theory (ISIT)*, Barcelona, Spain, Jul. 2016, pp. 865–869.

[37] A. Guo, Y. Zhong, W. Zhang, and M. Haenggi, "The Gauss-Poisson process for wireless networks and the benefits of cooperation," *IEEE Trans. on Commun.*, vol. 64, pp. 1916–1929, May 2016.

[38] F. Zabini, G. Pasolini, and A. Conti, "On random sampling with nodes attraction: The case of Gauss-Poisson process," in *Proc. of IEEE International Symposium on Information Theory (ISIT)*, Aachen, Germany, Jun. 2017, pp. 2278–2282.

[39] H. Shokri-Ghadikolaei, C. Fischione, G. Fodor, P. Popovski, and M. Zorzi, "Millimeter wave cellular networks: A MAC layer perspective," *IEEE Trans. on Commun.*, vol. 63, pp. 3437 – 3458, 2015.

[40] H. Shokri-Ghadikolaei and C. Fischione, "The transitional behavior of interference in millimeter wave networks and its impact on medium access control," *IEEE Trans. on Commun.*, vol. 64, pp. 723 – 740, 2016.

[41] M. Haenggi, *Stochastic geometry for wireless networks*. Cambridge University Press, 2012.

[42] P. Gupta and P. Kumar, "The capacity of wireless networks," *IEEE Trans. Information Theory.*, vol. 46, no. 2, pp. 388– 404, 2000.

[43] A. Iyer, C. Rosenberg, and A. Karnik, "What is the right model for wireless channel interference?" *IEEE Trans. Wireless Commun.*, vol. 8, p. 26622671, 2009.

[44] T. Bai and R. W. Heath, "Coverage and rate analysis for millimeter-wave cellular networks," *IEEE Trans. Wireless Commun.*, vol. 14, no. 2, pp. 1100–1114, Feb. 2015.

[45] M. Penrose, *Random geometric graphs*. Oxford University Press, 2003, no. 5.

[46] B. Blaszczyszyn and A. Giovanidis, "Optimal geographic caching in cellular networks," in *IEEE International Conference on Communications (ICC)*, June 2015, pp. 3358–3363.

[47] S. Biswas, S. Vuppala, and T. Ratnarajah, "On the performance of mmwave networks aided by wirelessly powered relays," *IEEE Journal of Selected Topics in Signal Processing*, vol. 10, no. 8, pp. 1522–1537, Dec. 2016.

[48] R. M. Corless, G. H. Gonnet, D. E. G. Hare, D. J. Jeffrey, and D. E. Knuth, "On the lambert w function," *Advances in Conputational Mathematics*, vol. 5, no. 1, pp. 329–359, 1996.

[49] H.-S. Jo, Y. J. Sang, P. Xia, and J. G. Andrews, "Heterogeneous cellular networks with flexible cell association: A comprehensive downlink SINR analysis," *IEEE Trans. Wireless Commun.*, vol. 11, no. 10, pp. 3484–3495, Oct. 2012.

[50] H. ElSawy and E. Hossain, "A modified hard core point process for analysis of random CSMA wireless networks in general fading

environments," *IEEE Trans. Commun.*, vol. 61, no. 4, pp. 1520 – 1534, April 2013.
[51] W. Lu and M. D. Renzo, "Performance analysis of relay aided cellular networks by using stochastic geometry," in *Proc. IEEE* 19^{th} *International Workshop on Computer Aided Modeling and Design of Communication Links and Networks*, Athens, Greece, Dec. 2014.
[52] M. D. Renzo and W. Lu, "End-to-end error probability and diversity analysis of AF-based dual-hop cooperative relaying in a Poisson field of interferers at the destination," *IEEE Trans. Wireless Comm.*, vol. 4, no. 1, pp. 15 – 32, Jan. 2015.
[53] A. Behnad, A. M. Rabiei, and N. C. Beaulieu, "Performance analysis of opportunistic relaying in a Poisson field of amplify-and-forward relays," *IEEE Trans. Communications.*, vol. 61, no. 1, pp. 97–107, Jan. 2013.
[54] A. Hasan and J. G. Andrews, "The guard zone in wireless ad hoc networks," *IEEE Trans. Wireless Comm.*, vol. 4, no. 3, pp. 897–906, March 2007.
[55] H. Q. Nguyen, F. Baccelli, and D. Kofman, "A stochastic geometry analysis of dense IEEE 802.11 networks," in *IEEE International International Conference on Computer Communications*, Barcelona, Spain, May 2007, pp. 1199–1207.
[56] M. Haenggi, "Mean interference in hard-core wireless networks," *IEEE Commun. Lett.*, vol. 15, no. 8, pp. 792–794, Aug. 2011.
[57] ——, *Stochastic Geometry for Wireless Networks*. Cambridge University Press, 2012.

Satyanarayana Vuppala (S'12-M'17) received the B.Tech. degree with distinction in Computer Science and Engineering from JNTU Kakinada, India, in 2009, and the M.Tech. degree in Information Technology from the National Institute of Technology, Durgapur, India, in 2011. He received the Ph.D. degree in Electrical Engineering from Jacobs University Bremen in 2014. He is currently a postdoctoral researcher at Interdisciplinary Centre for Security, Reliability and Trust (SnT), University of Luxembourg. His main research interests include 5G networks, Millimeterwave communications, and Edge caching. He also work on physical, access, and network layer aspects of wireless security. He is a recipient of MHRD, India scholarship during the period of 2009-2011.

Thang X. Vu (S'11–M'15) was born in Hai Duong, Vietnam. He received the B.S. and the M.Sc., both in Electronics and Telecommunications Engineering, from the VNU University of Engineering and Technology, Vietnam, in 2007 and 2009, respectively, and the Ph.D. in Electrical Engineering from the University Paris-Sud, France, in 2014.

From 2007 to 2009, he was with the Department of Electronics and Telecommunications, VNU University of Engineering and Technology, Vietnam as a research assistant. In 2010, he received the Allocation de Recherche fellowship to study Ph.D. in France. From September 2010 to May 2014, he was with the Laboratory of Signals and Systems (LSS), a joint laboratory of CNRS, CentraleSupelec and University Paris-Sud XI, France. From July 2014 to January 2016, he was postdoctoral researcher with the Information Systems Technology and Design (ISTD) pillar, Singapore University of Technology and Design (SUTD), Singapore. Currently, he is research associate at Interdisciplinary Centre for Security, Reliability and Trust (SnT), University of Luxembourg. His research interests are in the field of wireless communications, with particular interests of cache-assisted 5G, Machine learning -aided communications networks, cloud radio access networks, resources allocation and optimization, cooperative diversity and channel/network coding.

Sumit Gautam (S'14) received the B.Tech. degree (Hons.) in electronics and communication engineering from the LNM Institute of Information Technology (Deemed University), Jaipur, Rajasthan, India in 2013 and the MS degree in electronics and communication engineering by research from the International Institute of Information Technology (Deemed University), Hyderabad, Telangana, India in 2017. He is currently pursuing the Ph.D. degree in computer science from the Interdisciplinary Centre for Security, Reliability, and Trust (SnT), University of Luxembourg, Luxembourg. His research interests include simultaneous wireless transmission of information and energy (Wi-TIE), caching, optimization methods, and cooperative communications.

Symeon Chatzinotas (S'06-M'09-SM'13) is currently the Deputy Head of the SIGCOM Research Group, Interdisciplinary Centre for Security, Reliability, and Trust, University of Luxembourg, Luxembourg and Visiting Professor at the University of Parma, Italy. He received the M.Eng. degree in telecommunications from the Aristotle University of Thessaloniki, Thessaloniki, Greece, in 2003, and the M.Sc. and Ph.D. degrees in electronic engineering from the University of Surrey, Surrey, U.K., in 2006 and 2009, respectively. He was involved in numerous Research and Development projects for the Institute of Informatics Telecommunications, National Center for Scientific Research Demokritos, the Institute of Telematics and Informatics, Center of Research and Technology Hellas, and the Mobile Communications Research Group, Center of Communication Systems Research, University of Surrey. He has over 300 publications, 2500 citations, and an H-Index of 27 according to Google Scholar. His research interests include multiuser information theory, co-operative/cognitive communications, and wireless networks optimization. He was a co-recipient of the 2014 Distinguished Contributions to Satellite Communications Award, and the Satellite and Space Communications Technical Committee, the IEEE Communications Society, and the CROWNCOM 2015 Best Paper Award.

Bjrn Ottersten was born in Stockholm, Sweden, in 1961. He received the M.S. degree in electrical engineering and applied physics from Linkping University, Linkping, Sweden, in 1986, and the Ph.D. degree in electrical engineering from Stanford University, Stanford, CA, USA, in 1990. He has held research positions with the Department of Electrical Engineering, Linkping University, the Information Systems Laboratory, Stanford University, the Katholieke Universiteit Leuven, Leuven, Belgium, and the University of Luxembourg, Luxembourg. From 1996 to 1997, he was the Director of Research with ArrayComm, Inc., a start-up in San Jose, CA, USA, based on his patented technology. In 1991, he was appointed a Professor of signal processing with the Royal Institute of Technology (KTH), Stockholm, Sweden. From 1992 to 2004, he was the Head of the Department for Signals, Sensors, and Systems, KTH, and from 2004 to 2008, he was the Dean of the School of Electrical Engineering, KTH. He is currently the Director for the Interdisciplinary Centre for Security, Reliability and Trust, University of Luxembourg. As Digital Champion of Luxembourg, he acts as an Adviser to the European Commission.

He was a recipient of the IEEE Signal Processing Society Technical Achievement Award in 2011 and the European Research Council advanced research grant twice, in 2009-2013 and in 2017-2022. He has co-authored journal papers that received the IEEE Signal Processing Society Best Paper Award in 1993, 2001, 2006, and 2013, and seven other IEEE conference papers best paper awards. He has served as Editor-in-Chief of EURASIP Signal Processing Journal, Associate Editor for the IEEE TRANSACTIONS ON SIGNAL PROCESSING and the Editorial Board of the IEEE Signal Processing Magazine. He is currently a member of the editorial boards of EURASIP Journal of Advances Signal Processing and Foundations and Trends of Signal Processing. He is a fellow of IEEE and EURASIP.